Manganese-doped bismuth vanadate solid electrolytes.

Part 2.†—Electrical conductivity of $Bi_2V_{1-x}Mn_xO_{5.5-x}$

Longbao Qiu, Yuemei L. Yang and Allan J. Jacobson*

Department of Chemistry, University of Houston, Houston, TX 77204-5641, USA

The total electrical conductivities of a series of manganese-substituted bismuth vanadates, ($Bi_2V_{1-x}Mn_xO_{5.5-x}$; $0.15 \leqslant x \leqslant 0.25$) with the tetragonal ($\gamma$) structure have been measured using two-probe ac impedance spectroscopy. The conductivity data do not show simple Arrhenius behaviour. A linear variation of $\log(\sigma T)$ *vs.* $1/T$ is observed at low and high temperatures but at intermediate temperatures some curvature is apparent in the data, particularly when $x = 0.2$. Changes in conductivity with $p(O_2)$ indicate that the materials have mixed conductivity. Activation energies and pre-exponential factors for the linear regions have been determined for selected compositions at various $p(O_2)$ values. The total conductivity varies little with the extent of substitution of V by Mn. The results are compared with data for other γ-BIMEVOX systems.

Bismuth vanadate, $Bi_2VO_{5.5}$, has three structurally related phases: α, β and γ.[1,2] In air, these phases have been shown by high-temperature X-ray diffraction[2] to be stable at $T < 430\,^{\circ}C$ for α, $430\,^{\circ}C < T < 600\,^{\circ}C$ for β, and $T > 600\,^{\circ}C$ for γ. The phase transition temperatures reported in the literature vary somewhat due to hysteresis effects. The oxygen vacancies are ordered in the α and β phases and disordered over the oxygen atom positions in the vanadium oxygen layers in the γ phase.[2] The highest oxygen ion conductivity and the lowest activation energy are found for the disordered γ phase. Abraham *et al.*[3] and subsequently other research groups[4–17] have shown that partial substitution of the vanadium atoms in the parent compound $Bi_2VO_{5.5}$ by other metal atoms extends the temperature range over which the γ phase is stable. Suppression of the vacancy ordering enhances the ionic conductivity at lower temperature. To date, the conductivities of bismuth vanadates partially substituted with Cu,[3–10] Ni,[3,6,7] Co,[5,11] Zn,[10] Ti,[8–10,13] Sb,[5,12] Nb,[8,9,12] Pb,[8,9,14] Zr,[8,9,13] Ta,[8,9] Sn,[13] W,[15] Ge,[16] Fe[17] and Cr,[17] have been described. By far the most systematic and extensive conductivity studies have been made on $Bi_2V_{1-x}Cu_xO_{5.5-y}$. Enhanced conductivities for all metal substituents are observed below the γ to β transition temperature when the γ phase is stabilized. Results obtained with coupled substitutions of two metals have also been reported.[18] Conductivity measurements along defined crystal orientations in single crystals of $Bi_2VO_{5.5}$,[2] $Bi_2V_{1-x}Cu_xO_{5.5-y}$ and $Bi_2V_{1-x}Ni_xO_{5.5-y}$[6] have shown that the ionic conductivity along the *c* axis, *i.e.* normal to the $(Bi_2O_2)^{2+}$ and $(VO_{3.5}\square_{0.5})^{2-}$ sheets, is two to three orders of magnitude lower than the conductivity in the *ab* plane. Transport of the oxygen vacancies in the perovskite-like $(VO_{3.5}\square_{0.5})^{2-}$ layers is presumed to be responsible for the observed high ionic conductivity.

We have studied recently the Mn-doped $Bi_2VO_{5.5}$ phases which form the γ structure in the composition range $0.10 \leqslant x \leqslant 0.25$. The synthesis, thermal and magnetic measurements, and structural characterization of this series of compositions were reported in the preceding paper.[19] In the present paper, we describe the results of two-probe ac impedance measurements of the total conductivity of the manganese-substituted bismuth vanadates. Oxygen permeation and transport number measurements for one particular composition, $Bi_2V_{0.8}Mn_{0.2}O_{5.3}$, will be reported in a future publication.

Experimental

Polycrystalline samples of $Bi_2V_{1-x}Mn_xO_{3.5-x}$ ($0.15 \leqslant x \leqslant 0.25$) were prepared *via* the melt crystallization and annealing procedure reported previously.[19] Powder samples were ball-milled in ethanol for 3 days before pressing into pellets for conductivity measurements. For the measurements, pellets with thickness < 5 mm were prepared by uniaxial hydraulic pressing, while pellets with thickness $\geqslant$ 5 mm were prepared by cold isostatic pressing. The diameter of the pellets was approximately 7 mm. The pellets were sintered at 870 °C for 5 h at a heating and cooling rate of 2 °C min^{-1}. The measured densities corresponded to *ca.* 90% of the theoretical values calculated assuming the measured cell constants.[19] Both flat surfaces of the pellets were polished and coated with Engelhard 6926 platinum paste in order to establish good electrical contacts with the leads from the impedance analyser.

An HP 4192A impedance analyser interfaced to a personal computer was used in a two-probe configuration for the total electrical conductivity measurements. Conductivity data were obtained for compositions $x = 0.15$, 0.20 and 0.25 at oxygen partial pressures $p(O_2) = 1.0$, 0.21 and 3×10^{-4} atm, obtained using mixtures of predried oxygen and nitrogen. The $p(O_2)$ was regulated during each experiment with MKS 247C mass flow controllers and monitored with an Ametek TM-1B oxygen analyser. At each chosen oxygen partial pressure and temperature, the pellets were held isobarically and isothermally for 1–16 h before the final conductivity measurement was made. The actual equilibration time was dependent on the time needed to reach a constant conductivity reading. Generally the equilibration was *ca.* 1–4 h under $p(O_2) = 1.0$ and 0.21 atm. However, much longer equilibration times were needed under more reducing conditions. Conductivity data were obtained on heating and cooling in the range 125–720 °C for most of the samples. Thicker samples were used to increase the total resistance so that the measuring temperature could be raised to 800 °C. The temperature was increased and decreased in increments of 50 °C. Points taken during cooling were typically offset by 25 °C from the data obtained during heating in order to better define the Arrhenius plots. For each measurement, the impedance analyser scanned from 5 Hz to 13 MHz.

Results

The general features of the impedance spectra and their evolution with temperature are similar for all of the compositions studied. At low temperature, the impedance spectra consisted of one semicircle. Contributions from the bulk sample and grain boundaries could not be distinguished, although some spectra did show asymmetry on the low-frequency side, suggesting a grain boundary contribution. As the temperature

† Part 1, preceding paper.

increases, the resistance decreases and higher frequencies are required to measure complete semicircles due to the total conductivity (bulk + grain boundary contributions). Since the available maximum frequency of the impedance analyser is fixed, the semicircle corresponding to the bulk conductivity disappears on the high-frequency side. At the highest temperatures, only a spike at very low frequencies associated with polarization of the Pt electrodes is observed.[4,16] The low-frequency spike suggests that the compound is primarily an ionic conductor.[16] The total sample resistance at each temperature was determined from the intersection point of the spectrum with the real axis and converted into conductivity using $\sigma = l/AR$, where l is the pellet thickness and A is the pellet cross-sectional area.

Detailed conductivity studies were carried out for the $x = 0.20$ composition. In these studies, four pellets with thicknesses of 1.8, 2.6, 4.5 and 16.2 mm were used for the conductivity measurements. By varying the pellet thickness, the results were shown to scale with the geometric factor of the sample and the experimental procedure found to be consistent and repeatable. The experimental data are presented in the form of Arrhenius plots. Quantitative values of the activation energies, E_a, and pre-exponential factors, σ_0, were extracted from the data. The conductivity data were collected on both heating and cooling cycle(s).

The data for $x = 0.20$ measured with a 16.2 mm pellet are shown in Fig. 1 as plots of log (σT) *vs.* $10^3/T$. The data do not show simple Arrhenius-type behaviour with a single activation energy. The curves consist of two linear regions with different E_a, one at temperatures $>636\,^{\circ}C$ $(10^3/T < 1.1)$ and the other below $315\,^{\circ}C$ $(10^3/T > 1.7)$. In the intermediate temperature region, a pronounced curvature is also present in the data. For the linear regions, E_a and σ_0 were derived by fitting the experimental data to the Arrhenius equation and are summarized in Table 1.

In Fig. 1(a) all of the data at $p(O_2) = 1.0$ atm measured on cooling fall on a line drawn through the points measured on heating. Similar behaviour can be seen in Fig. 1(b) at $p(O_2) = 0.21$ atm but only in the temperature ranges where the variation is linear. In the transition region considerable hysteresis was observed between different heating and cooling cycles. Some correlation was observed between the magnitude of the hysteresis and the maximum measurement temperature. The activation energies, E_a, for the two linear regions are nearly equal, 69.0 $(10^3/T > 1.7)$ *vs.* 67.3 kJ mol^{-1} $(10^3/T < 1.1)$, at $p(O_2) = 1.0$ atm whereas corresponding values of 72.7 *vs.* 64.4 kJ mol^{-1} are obtained at $p(O_2) = 0.21$ atm. The data points shown in Fig. 1(c) obtained under more reducing conditions, $p(O_2) = 3 \times 10^{-4}$ atm, are different for the first heating and subsequent heating and cooling cycles. The conductivities measured on the first heating cycle in the low and intermediate temperature ranges are higher than the data obtained on cooling. On the second cycle, however, the data obtained on heating and cooling fall on the same line, and both sets of data points agree very well with the cooling data measured on the first cycle. No hysteresis effects are observed after the first heating cycle. The results suggest that a compositional change occurs under reducing conditions, and that equilibrium is established during the time of the experiment only at high temperature. The data in Fig. 1(c) show an intermediate region similar to those observed in the conductivity data at higher oxygen partial pressures, the curvature, however, is less pronounced. The activation energies corresponding to the two linear regions are 60.2 $(10^3/T > 1.7)$ and 55.6 kJ mol^{-1} $(10^3/T < 1.1)$.

Qualitatively similar behaviour was observed for the compositions with $x = 0.15$ and 0.25. The results for $x = 0.25$ are shown in Fig. 2. The conductivity data do not show simple Arrhenius behaviour and the curves again consist of two linear regions with different E_a, one at $T > 636\,^{\circ}C$ $(10^3/T < 1.1)$ and the other below $496\,^{\circ}C$ $(10^3/T > 1.3)$. An intermediate non-linear region was observed between the two linear regions at each of the three partial oxygen pressures. The intermediate region is much less pronounced in the $x = 0.25$ than in the $x = 0.20$ data, and is similar at each of the three oxygen pressures.

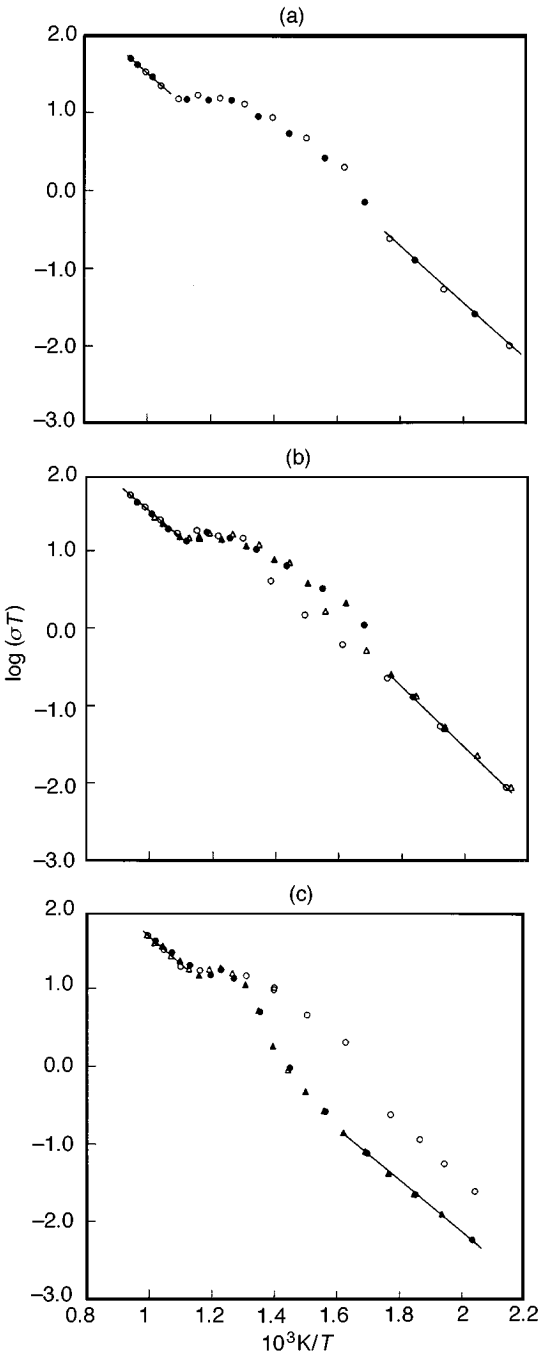

Fig. 1 Total electrical conductivity for $Bi_2V_{0.80}Mn_{0.20}O_{5.40}$, $l = 16.2$ mm, $A = 21.31$ mm^2. ○, First heating data; ●, first cooling data; △, second heating data; ▲, second cooling data. (a) $p(O_2) = 1.0$ atm; (b) $p(O_2) = 0.21$ atm; (c) $p(O_2) = 3 \times 10^{-4}$ atm.

Table 1 Summary of the conductivity data for $Bi_2V_{0.80}Mn_{0.20}O_{5.40}$

$p(O_2)$/atm	$10^3/T$ range	σ_0/S cm^{-1}	E_a/kJ mol^{-1}
3×10^{-4}	>1.7	1.55×10^4	60.2
	<1.1	3.62×10^4	55.6
0.21	>1.7	1.24×10^6	72.7
	<1.1	7.5×10^4	64.4
1.0	>1.7	5.93×10^5	69.0
	<1.1	1.08×10^5	67.3

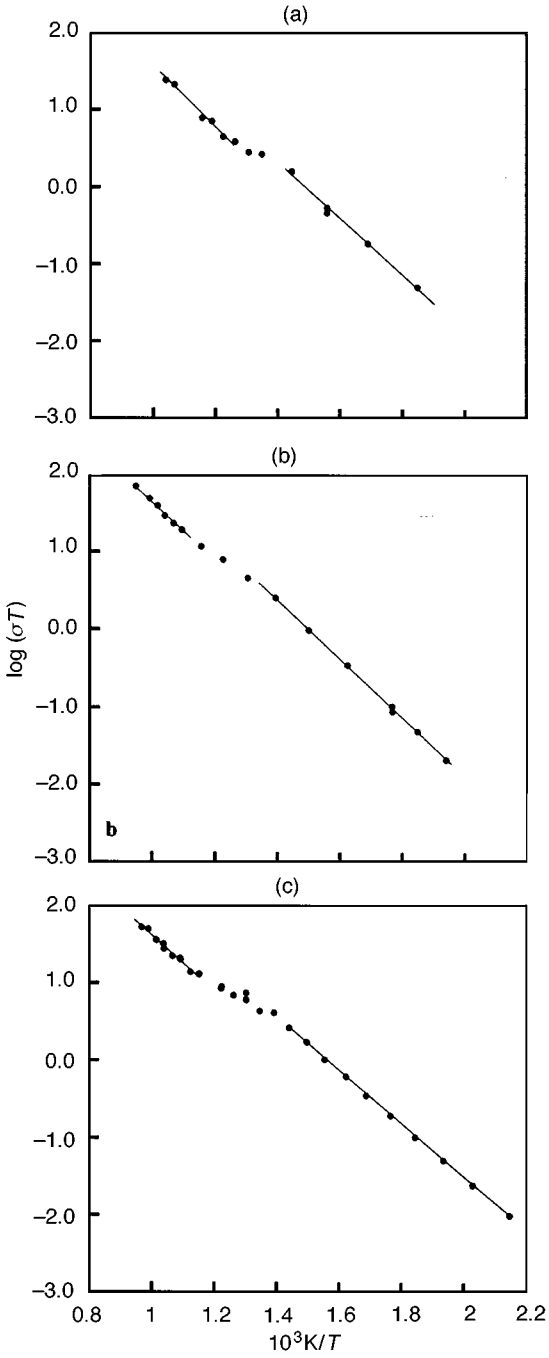

Fig. 2 Total electrical conductivity for $Bi_2V_{0.75}Mn_{0.25}O_{5.25}$, $l=18.4$ mm, $A=25.93$ mm^2. (a) $p(O_2)=1.0$ atm; (b) $p(O_2)=0.21$ atm; (c) $p(O_2)=3\times10^{-4}$ atm.

The results for $x=0.15$ are closely similar to those for $x=0.25$. A comparison of the conductivity data for the three different compositions is shown in Fig. 3. The activation energies and pre-exponential factors corresponding to the two linear regions in the data for $x=0.15$ and 0.25 are summarized in Tables 2 and 3.

The dependence of the total electrical conductivity on $p(O_2)$ is small for each of the compositions studied. In the high-temperature region, a small increase in conductivity is observed when $p(O_2)$ is lowered to 3×10^{-4} atm but little difference is observed between the values measured at $p(O_2)=1$ and 0.21 atm. At lower temperatures, the conductivities increase by a small amount from $p(O_2)=1$ to 0.21 atm but the behaviour at $p(O_2)=3\times10^{-4}$ atm is complicated by the cycling effect noted above [Fig. 1(c)]. For the sample with $x=0.2$ which had reached equilibrium, the low-temperature conductivity is lower

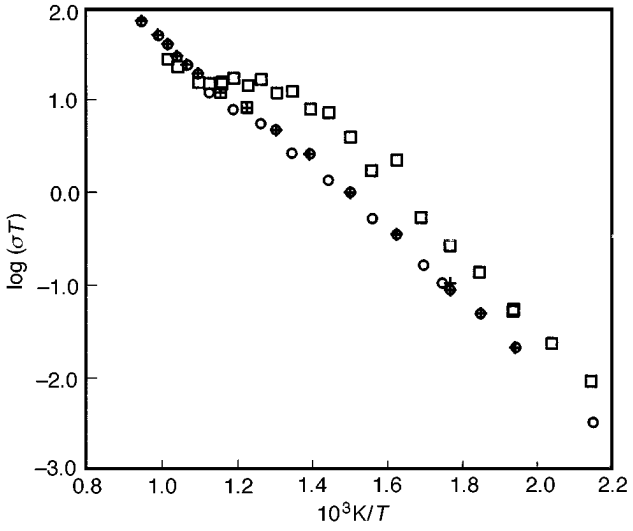

Fig. 3 Comparison of the conductivities of $Bi_2V_{1-x}Mn_xO_{5.5-x}$ for $x=0.15$ (○), 0.20 (□) and 0.25 (+) at $p(O_2)=0.21$ atm. ($l=15.0$ mm, $A=14.3$ mm^2 for the sample with $x=0.15$).

Table 2 Summary of the conductivity data for $Bi_2V_{0.85}Mn_{0.15}O_{5.35}$

$p(O_2)$/atm	$10^3/T$ range	σ_0/S cm^{-1}	E_a/kJ mol^{-1}
3×10^{-4}	>1.3	1.45×10^5	64.0
	<1.1	5.29×10^5	78.2
0.21	>1.3	2.75×10^5	69.8
	<1.1	3.74×10^5	75.2
1.0	>1.3	1.23×10^5	65.6
	<1.1	2.71×10^5	74.4

Table 3 Summary of the conductivity data for $Bi_2V_{0.75}Mn_{0.25}O_{5.25}$

$p(O_2)$/atm	$10^3/T$ range	σ_0/S cm^{-1}	E_a/kJ mol^{-1}
3×10^{-4}	>1.4	2.20×10^5	65.2
	<1.1	1.63×10^5	68.6
0.21	>1.4	4.61×10^5	72.3
	<1.1	4.29×10^5	76.1
1.0	>1.4	1.08×10^5	65.2
	<1.1	3.67×10^5	76.5

at $p(O_2)=3\times10^{-4}$ atm than at the higher oxygen partial pressures.

The dependence of conductivity data on x is rather complex. At low temperature the maximum conductivity is observed at $x=0.20$. The conductivity of the $x=0.15$ and 0.25 compositions increases faster with temperature than that of the $x=0.20$ sample, so that at 593 °C and 693 °C the conductivities of the three compositions are almost equal. The weak dependence of the conductivity on the concentration of the substituent, in this case manganese, is observed in most BIMEVOX systems.

Discussion

The conductivity data for each of the $Bi_2V_{1-x}Mn_xO_{5.5-x}$ compositions investigated show similar features. Specifically, the conductivity does not show simple Arrhenius behaviour and is characterized by two linear parts separated by an intermediate non-linear region. The deviation from non-linear behaviour varies both with composition and with the oxygen partial pressure.

Two distinct activation energies have been reported in several previous studies of the conductivity of γ phases stabilized with different metal substituents. For example, Lazure *et al.*[5] reported values of 43.9 and 61.9 kJ mol^{-1} for BICOVOX (average of the four compositions studied), Pernot *et al.*[6] gave 44.8 and 53.1 kJ mol^{-1} for in-plane measurements on a

BINIVOX single crystal ($x=0.07$) and Joubert *et al.* reported 34.7 and 59.8 kJ mol^{-1} for BINBVOX ($x=0.25$).[12] In each case, the lower activation energy refers to the higher temperature region. The change in activation energy has been attributed to a phase transition in which partially ordered oxygen vacancies become disordered. This transition is evident in X-ray diffraction studies of BICUVOX single crystals which show the disappearance of incommensurate superlattice reflections corresponding approximately to a $3a\times3b\times c$ unit cell at 510 °C.[6] The low- and high-temperature phases have been designated γ' and γ by the previous workers. Above the $\gamma'\rightarrow\gamma$ phase transition, the activation energies reported for different metal-substituted systems are similar and in the range 37–46 kJ mol^{-1}. At temperatures below the phase transition, significant variations in activation energies have been observed. For example, Krok *et al.*[20] reported values in the range 59.8 to 69.4 kJ mol^{-1} for $x=0.1$ samples of BICUVOX that were prepared differently. Similar differences were observed in single crystals of BICUVOX ($x=0.12$)[6] and polycrystalline BICOVOX.[11]

In a previous paper, we described transmission electron microscopy studies of two samples of $Bi_2V_{0.85}Mn_{0.15}O_{5.35}$, one which was quenched from 850 °C and the other slow cooled. The results are consistent with previous single-crystal XRD observations and show well developed superlattice reflections in the cooled sample and much less well developed order in the quenched sample suggesting that a $\gamma'\rightarrow\gamma$ transition takes place at higher temperature. The manganese system, however, shows two important differences from other systems. First, none of the measured activation energies are as low as those observed for other BIMEVOXs (37–46 kJ mol^{-1}) in the high-temperature region. Secondly, the slopes of the Arrhenius plots show a substantial deviation from linearity at intermediate temperatures and hysteresis effects are observed. Similar deviations from Arrhenius behaviour have been observed in single-crystal BICUVOX ($x=0.07$).[6] These observations suggest that some other mechanism contributes to the activation energy and hysteresis in the Mn case.

The general shape of the transition from the low-temperature to the high-temperature region, particularly for $x=0.2$, is reminiscent of the behaviour observed in the ionic conductivity of some glasses.[21] In the Mn system at low temperatures, the combined effects of the Mn–V atom distribution, displacement disorder and the oxygen vacancy distribution may produce a glass-like state of different Mn–O–V–O_V configurations. At low temperatures, the activation energy has contributions from both the generation of mobile vacancies (the vacancies are ordered in the low-temperature γ' structure) and their migration. Above a temperature that corresponds to a glass-transition temperature, local structure deformations can occur that involve metal atom displacements. These local deformations facilitate transfer of a vacancy to a neighbouring position and lead to an enhancement in the conductivity. Conversion of square-pyramidal VO_5 to tetrahedral VO_4 units or MnO_6 octahedra to MnO_5 square pyramids in different Mn,V–O atom cluster arrangements are examples of transformations that require local metal atom displacements. At sufficiently high temperatures, the vacancies become completely disordered ($\gamma'\rightarrow\gamma$ transition) and normal Arrhenius behaviour is recovered.

The variation of the conductivities with the extent of manganese substitution is shown in Fig. 3. As observed for other BIMEVOX systems the changes are small. Below 500 °C the highest value is observed at $x=0.2$ but at higher temperatures the results are very similar. The changes in the total electrical conductivities with changes in $p(O_2)$ are small and are related both to the partial reduction of Mn^{3+} to Mn^{2+} and to the introduction of some degree of electronic conductivity. We have shown previously by thermogravimetric and magnetic measurements that significant reduction of Mn^{3+} to Mn^{2+} occurs in air when samples are heated above 800 °C. The electronic contribution to the total conductivity has been determined for one specific composition, $x=0.20$, by oxygen permeation and transport number measurements and will be described in a subsequent paper.[23] The electronic conductivity estimated from oxygen permeation fluxes is approximately 7% of the total conductivity at 850 °C. Electronic contributions to the total conductivity with similar magnitudes have been reported previously for Cu and Ni substituted systems by Iharada *et al.*[7]

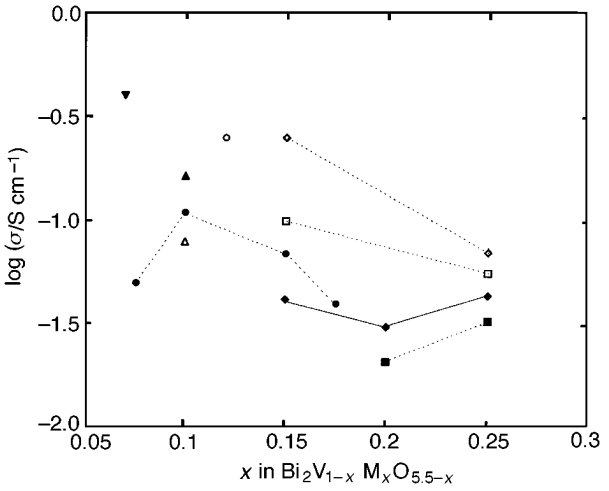

Fig. 4 Comparison of BIMEVOX conductivities at 1000 K. ●, Co (ref. 5); ■, Fe (ref. 17); ◆, Mn (this work); ▲, Cu (ref. 4); ▼, Ni (ref. 6); ○, Cu (ref. 6); □, Nb (ref. 12); ◇, Sb (ref. 12); △, La (ref. 22).

The results for the $Bi_2V_{1-x}Mn_xO_{5.5-x}$ series are compared in Fig. 4 at 1000 K with data for a number of other systems reported in the literature. At 1000 K, the highest values are observed for Ni and Cu systems measured in the *ab* plane on single crystals and for Sb ($x=0.15$). The data span a range of approximately one order of magnitude. The conductivities of the manganese samples are at the lower end of the range and are very similar to the recently reported results for $Bi_2V_{1-x}Fe_xO_{5.5-x}$.[17]

Summary and Conclusions

The total electrical conductivities of $Bi_2V_{1-x}Mn_xO_{5.5-x}$ ($0.15\leqslant x\leqslant0.25$) samples have been measured using ac impedance spectroscopy as a function of temperature at various oxygen partial pressures. Detailed studies reveal significant departures from Arrhenius behaviour and hysteresis effects. A significant curvature at intermediate temperature range is observed between two linear regions at low and high temperature. The conductivity data show little dependence on x and the measured values are comparable to those recently reported for the γ phases in the same composition range stabilized with Fe^{3+}.[17]

We thank the Robert A. Welch Foundation and the Texas Center for Superconductivity at the University of Houston (TCSUH) for financial support of this work. We thank Mr. Deva Ponnusamy at TCSUH for his help with the cold isostatic pressing.

References

1 F. Abraham, M. F. Debreuille-Gresse, G. Mairesse and G. Nowogrocki, *Solid State Ionics*, 1988, **28/30**, 529.
2 R. N. Vannier, G. Mairesse, F. Abraham, G. Nowogrocki, E. Pernot, M. Anne, M. Bacmann, P. Strobel and J. Fouletier, *Solid State Ionics*, 1995, **78**, 183.

3 F. Abraham, J. C. Boivin, G. Mairesse and G. Nowogrocki, *Solid State Ionics*, 1990, **40/41**, 934.
4 J. R. Dygas, F. Krok, W. Bogusz, P. Kurek, K. Reiselhuber and M. W. Breiter, *Solid State Ionics*, 1994, **70/71**, 239.
5 S. Lazure, R. N. Vannier, G. Nowogrocki, G. Mairesse, C. Muller, M. Anne and P. Strobel, *J. Mater. Chem.*, 1995, **5**, 1395.
6 E. Pernot, M. Anne, M. Bacmann, P. Strobel, J. Fouletier, R. N. Vannier, G. Mairesse, F. Abraham and G. Nowogrocki, *Solid State Ionics*, 1994, **70/71**, 259.
7 T. Iharada, A. Hammouche, J. Fouletier, M. Kleitz, J. C. Boivin and G. Mairesse, *Solid State Ionics*, 1991, **48**, 257.
8 J. B. Goodenough, A. Manthiram, M. Paranthaman and Y. S. Zhen, *Solid State Ionics*, 1994, **52**, 105.
9 J. B. Goodenough, A. Manthiram, M. Paranthaman and Y. S. Zhen, *Mater. Sci. Eng. B*, 1992, **12**, 357.
10 V. Sharma, A. Shukla and J. Gopalakrishnan, *Solid State Ionics*, 1992, **58**, 359.
11 F. Krok, W. Bogusz, W. Jakubowski, J. R. Dygas and D. Bangobango, *Solid State Ionics*, 1994, **70/71**, 211.
12 O. Joubert, A. Jouanneaux, M. Ganne, R. N. Vannier and G. Mairesse, *Solid State Ionics*, 1994, **73**, 309.
13 J. Yan and M. Greenblatt, *Solid State Ionics*, 1995, **81**, 225.
14 R. N. Vannier, G. Mairesse, G. Nowogrocki, F. Abraham and J. C. Boivin, *Solid State Ionics*, 1992, **53/56**, 713.
15 R. N. Vannier, G. Mairesse, F. Abraham and G. Nowogrocki, *Solid State Ionics*, 1995, **80**, 11.
16 C. K. Lee, M. P. Tan and A. R. West, *J. Mater. Chem.*, 1994, **4**, 525.
17 O. Joubert, M. Ganne, R. N. Vannier and G. Mairesse, *Solid State Ionics*, 1996, **83**, 199.
18 R. N. Vannier, G. Mairesse, F. Abraham and G. Nowogrocki, *Solid State Ionics*, 1994, **70/71**, 248.
19 Y. L. Yang, L. Qiu, W. T. A. Harrison, R. Christoffersen and A. J. Jacobson, preceding paper.
20 F. Krok, W. Bogusz, P. Kurek, M. Wasiucionek, W. Jakubowski and J. R. Dygas, *Mater. Sci. Eng.*, 1993, **B21**, 70.
21 J. L. Souquet, M. Levy and M. Duclot, *Solid State Ionics*, 1994, **70/71**, 337.
22 C. K. Lee, B. H. Bay and A. R. West, *J. Mater. Chem.*, 1996, **6**, 331.
23 Y. L. Yang, L. Qiu and A. J. Jacobson, *J. Mater. Chem.*, submitted for publication.

Paper 6/04693B; *Received* 4*th July*, 1996